Conventional matrix CHCA overlayed on graphene enhances MALDI-TOF/TOF signal: its application to improve detection of phosphorylated peptides.

Carlos E. Rodríguez[1], Javier Palacios[1], Ignacio Fajardo[2,3], José Luis Urdiales[2,3], Xavier Le Guével[5], José Lozano[,2,4], Francisca Sánchez-Jiménez[2,3]

[1]Proteomics Unit of the Supercomputing and Bioinnovation Center of the University of Málaga. Parque Tecnológico de Andalucía, Málaga, Spain.

[2] Department of Molecular Biology and Biochemistry, University of Malaga. Málaga, Spain.

[3]Unit 741 of "Centro de Investigación en Red en Enfermedades Raras" (CIBERER-ISCIII). Malaga, Spain.

[4]Laboratorio de Oncología Molecular, Servicio de Oncología Médica, Instituto de Biomedicina de Málaga (IBIMA), Hospital Universitario Virgen de la Victoria, Málaga, Spain

[5]Therapeutic Nanosystem, Andalusian Centre for Nanomedicine and Biotechnology (BIONAND) "Parque Tecnológico de Andalucía", Campanillas, Málaga, Spain.

Abbreviations

CHCA, α-cyano-4-hydroxycinnamic acid; PSD, post-source decay; CID, collision induced dissociation; Nd:YAG, neodymium-doped yttrium aluminium garnet; Calmix, 4700 Proteomics Analyzer Calibration Mixture; Au NCs, gold nanoclusters; GSH, Glutathione; Zw, Zwitterion; MALDI-TOF, Matrix assisted desorption ionization-time of flight; MS, mass spectrometry.

Introduction:

Ionization of analytes by MALDI-TOF mass spectrometry is based on the use of a matrix with an absorption spectrum in the range of the wavelength emitted by the laser. This resonant absorption of light favors the ablation and ionization of the matrix that transfers the charge to the co-crystalized molecules of the sample.

A conventional MALDI-TOF matrix should exhibit the following characteristics: i) a strong absorption in the selected laser emission wavelength ii) a low melting point to assist desorption and vaporization from the MALDI plate; and iii) a low molecular weight in order to minimize the interference in the measurement range.

In the last few years, the use of graphene as a new MALDI matrix for the analysis of low molecular weight molecules has been extensively described. The main advantage of this matrix is related to a spectra without interfering peaks in the low mass range, presents in the traditional matrices [2] and to an attenuation of analyte fragmentation attenuation [8], which might reduce the complexity of the spectra at higher signal intensities.

Graphene has ultrafast electron mobility with an efficient electron-phonon coupling, as well as frequency-independent optical absorption properties and a high thermal conductivity [13, 18, **Error! Reference source not found.**]. We speculate that the good adsorption of the peptides and other molecules in the planar structure of the graphene together with its exceptional optical and electronic properties could facilitate the ionization of the analytes. A higher

content of ionized analyte molecules with decreased vibrational energy during the laser ablation would lead to the improvement of signal, especially of those readily clevable species.

Following this hypothesis, the main objective of this work was to test the putative advantages of using graphene as co-matrix of α-cyano-4-hydroxycinnamic acid (CHCA) to combine the excellent electrical, optical, thermal and adsorbent properties of graphene with the intense resonant absorbtion of light of CHCA to enhance the signal in MALDI-TOF mass spectrometry.

The detection of the molecules that are easily fragmented by MALDI-TOF mass spectrometry is an underestimated problem. The desorption/ionization processes carried out by laser ablation of the sample produce a thermal agitation and that vibrational energy leads to the spontaneous fragmentation of the molecules. This effect is used in the PSD (post source decay) mode MS/MS analysis where the fragmentation ratio is simply improved by increasing the laser intensity. The phosphoester is a labile bond, so its detection could be missed even though is a group easily ionizable due to a high fragmentation rate. In our experience, the intensity of the MS/MS spectra of phosphorylated peptides is detected with a higher sensitivity than expected based on the peak height observed in the peptide mass fingerprinting spectra. This effect is more pronounced when the modified residue is serine or threonine due to the high prevalence of the neutral losses of 98 and 80 Da in both cases.

In this study, we focused on improving signals obtained in the analysis of complex peptidic samples and in the benefits of the stabilization effect of graphene to

enhance the signal of phosphopeptides that, in the habitual conditions, give rise to an easily fragmented group.

The association of the conventional matrices CHCA and sinapinic acid with graphene indeed showed a significant enhancement of the signal. The use of graphene as co-matrix may be of particular interest in the analysis of phosphorylated peptides, which show a selective enhancement of their signal due to the characteristics attenuation of the fragmentation, obtained with the use of this novel MALDImatrix.

Material and methods:

Matrices:

CHCA, sinapinic acid, acetonitrile and trifluoroacetic acid, ammonium bicarbonate and bovine serum albumin were purchased from Sigma-Aldrich (St. Louis, Mo., USA), ethanol and acetic acid were from Merck (VWR International) and the graphene was acquired from GRAPHENEA (San Sebastián, SPAIN).

CHCA was prepared as a saturated solution in 50% acetonitrile 0.1% TFA, Sinapinic acid as a saturated solution in 30% acetonitrile 0.1% TFA. One mg of the graphene powder was resuspended in 0.5 mL of 50% ethanol using a low power bath sonicator (Selecta Ultrasons, JP Selecta, Spain) for 3 minutes in a glass vial. Inmediatly after, 1 μL of the resuspended graphene was spotted onto the MALDI plate and dried with a hot air stream. Then, the sample and the matrix were added with the common protocol.

An UV-3100 PC spectrophotometer (VWR International) was used to set up the best conditions to prepare the graphene solution. For this purpose was measured the light absorption at 270 nm. Figure 1S of supplemental information shows the great difference between results obtained by performing the graphene sonication in glass vials and those obtained with plastic Eppendorfs. The characteristic wavelength absorption of graphene at 270 nm is highly increased employing glass vials. The sedimentation of the sample was also studied (figure 2S, supplemental information). After 45 min resting on the bench top only the background was decreased without a parallel decrease in the absorption at 270 nm. After enough time of sedimentation (overnight) or with forced sedimentation by centrifugation the signal almost completely dissapears; therefore, the graphene suspension in ethanol 50% must be sonicated for 2 minutes before each use.

Nanoclusters Synthesis procedure

Synthesis of AuZw. Thioctic-zwitterion (Zw) was synthesized following the protocols described elsewhere [20]. Au NCs with the ligand zwitterion (Zw) was prepared by the addition of gold salt ($HAuCl_4.3H_2O$, 50 mM) to a basic solution (pH 10.0) containing the ligand in the presence of the strong reducing agent $NaBH_4$ (50 mM) and stirred for 15 hours. AuZw was synthesized with the molar ratio Au:Zw:$NaBH_4$ = 1:10:2. Afterwards, solutions were filtered twice with Amicon 3 (3 kDa cut-off) filters at 13,600 rpm for 20 min to remove the excess of free ligand, concentrated to 500 μg/mL of gold in water and kept refrigerated at 4ºC until use.

Synthesis of AuGSH. Briefly, 326 μL of $HAuCl_4 \bullet 3H_2O$ (50mM) was added to 5 mL of glutathione (GSH) (1 mg/mL) stirred at 60°C for 5 hours and then cooled down at room temperature. AuGSH was synthesized with the molar ratio 1:1. Afterwards, the solution was centrifuged at 10,000 rpm for 10 min to remove the big aggregates. The yellowish supernatant containing the fluorescent nanoclusters was precipitated in a mixture water/ethanol (1/2 v/v) and the pellet was resuspended in water at pH 7.0 Following this, the solution was filtered twice with an Amicon 3 filter to remove the free glutathione. AuGSH solution was stable for months and kept refrigerated until use.

In vitro phosphorylation

Recombinant, FLAG-tagged KSR1 was immunopurified from quiescent 293T cells stably transfected with pCMVTag2b-KSR1 and subjected to an in vitro kinase assay with purified, active MAPK (Millipore, USA). Briefly, cell lysates were prepared in NP40 buffer and immunoprecipitated (250 μg) with 30 μl anti-FLAG resin (Sigma-Aldrich, USA), as described (Jagemann et al. 2008). Immunoprecipitates were previously dephosphorylated in vitro by treatment with 67 units of lambda phosphatase (Santa Cruz Biotechnology, Germany). The phosphatase was removed by extensive washing with kinase buffer A (25 mM Tris-Cl, pH 7.5, 0.02 mM EGTA) and KSR1 was phosphorylated in vitro by incubation with 20 ng activated MAPK in kinase buffer B (kinase buffer A plus 100 μM ATP and 10 mM MgAc) for 30 min at 30°C. Reactions were stopped by boiling in 1X Laemmli sample buffer and phosphorylated proteins were resolved by SDS-PAGE followed by Coomassie staining.

The excised bands were digested with the use of a DigestPro MS robot as described in the bibliography [15, 16]. Briefly, the excised spots were sequentially incubated for 15 min -discarding the solution in every step- with 90 μL of 50% ACN 25 mM ammonium bicarbonate (Sigma-Aldrich), 45 μL of 50 mM ammonium bicarbonate, followed by 45 μL of 100% acetonitrile twice. After discarding the acetonitrile, the spots were dried for additional 15 min. After thawing the stock of trypsin gold (PROMEGA, Madison, WI, USA) (1 μg/μL in 50 mM acetic acid, it was diluted 1:50 with 25 mM ammonium bicarbonate and the gels were rehydrated with 15 μL of the enzyme. The incubation was performed at 37°C for 4 hours. After the first 2 hours, 10 μL of Milli-Q water were added to compensate evaporation. The elution of the peptides from the gel was performed in two steps; the former in basic medium with 10 μL of 25 mM ammonium bicarbonate, the second by adding 20 μL of 5% (v/v) formic acid.

In solution digestion of casein (Sigma-Aldrich) was also carried out using the robot DigestPro MS. Ten μL of the sample (protein concentration: 50 ng/μL) was mixed with 10 μL of the following solution: 0.2% SDS 100 mM Tris-HCl (pH 8) 10 mM DTT, and incubated at 60°C for 45 min. Then, the plate temperature was set to 37°C and the solution was allowed to reach this temperature for 20 min. Then 20 μL of 50 mM ammonium bicarbonate was added to this solution. The frozen stock of trypsin gold -1 μg/μL in acetic acid 50 mM- was diluted 1:300 with 25 mM ammonium bicarbonate. Thus, 15 μL of the trypsin solution prepared was added to each reaction well to carry out the digestion of the samples. Finally, the reaction was stopped by adding 15 μL of 2.5% TFA.

The digested samples were desalted using ZipTip μ-C18 pipette tips (Millipore, Billerica, MA, USA) and directly spotted onto the MALDI plate with the DigestPro MS instrument. For this purpose, the ZipTip was activated dispensing to waste 20 μL of 100% acetonitrile, followed by 20 μL of 0.1% TFA. The sample was loaded by slow aspiration at 0.02 ml/min and dispensed to waste at 0.5 mL/min, then washed with 20 μL of 0.1% TFA and directly eluted onto the MALDI plate with 1 μL alpha-cyano-4-hydroxycinnamic acid matrix (5 mg/mL in 50% ACN 0.1% TFA).

Isolation, protein extraction and digestion of leukocytes

The frozen cell pellets of human leucocytes isolated by the ficoll method [14] were thawed and washed twice with PBS at 4°C. The last supernatant was discarded and the cell pellets were lysed with 20 μl of a 100 mM Tris 0.2% SDS 10 mM DTT buffer. The sample was heated for 45 min at 60°C and then fixed at a temperature of 37°C. Afterwards, 20 μl of 50 mM ammonium bicarbonate and 15 μl of diluted Trypsin Gold stock solution (that is, 1 μg/μl trypsin in 50 mM acetic acid 1:50 diluted with 25 mM ammonium bicarbonate) were added. After 90 minutes the reaction was stopped by adding 15 uL of 2.5% TFA. Samples were desalted using ZipTip C18.

Mass spectrometry

A 4700 Proteomics Analyzer Mass Spectrometer (ABSCIEX. Framingham, MA. USA) was used for the analyses. The samples were analyzed in the following ion modes: Reflector positive ion mode: 20 kV source 1 acceleration voltage. The Grid 1 voltage to source 1, Mirror 2 to Mirror 1 and Mirror 2 to source 1 were

respectivelly set to 70.50%, 143.45% and 101.99% of the source 1 acceleration voltage. Delay time DE1 was 500 ns, and the low mass gate was enabled with an offset of 0.0. Each data point was the summation of 40 spectra, acquired with 50 laser shots each. Internal calibration was carried out with a set of synthetic peptides (4700 Proteomics Analyzer Calibration Mixture, ABSCIEX).

Reflector negative ion mode: 20 kV source 1 acceleration voltage. The Grid 1 voltage to source 1, Mirror 2 to Mirror 1 and Mirror 2 to source 1 were respectively set to 70.00%, 143.66% and 102.00% of the source 1 acceleration voltage. Delay time DE1 was disabled, and the low mass gate was enabled with an offset of 0.0. Each data point was the summation of 40 spectra, acquired with 50 laser shots each. Internal calibration was carried out with a set of synthetic peptides (4700 Proteomics Analyzer Calibration Mixture, ABSCIEX).

Linear low mass positive ion mode: 20 kV source 1 acceleration voltage. The Grid 1 voltage was set to 94% of the source 1 acceleration voltage. Delay time DE1 was 420 ns, and the low mass gate was enabled with an offset of 0.0. Each data point was the summation of 20 spectra, acquired with 125 laser shots each. External calibration was carried out with a set of synthetic peptides (4700 Proteomics Analyzer Calibration Mixture, ABSCIEX).

Linear middle mass positive ion mode: 20 kV source 1 acceleration voltage. The Grid 1 voltage was set to 92.5% of the source 1 acceleration voltage. Delay time DE1 was 850 ns, and the low mass gate was enabled with an offset of 0.0. Each data point was the summation of 20 spectra, acquired with 50 laser shots each. External calibration was carried out with a set of synthetic peptides (Sequazyme Peptide Mass Standars Kit, Calibration Mixture 3, ABSCIEX).

Results:

Graphene has already been successfully employed as a MALDI-TOF matrix for the analyses of small molecules [8, 4, 2]. Also we were able to get signal with graphene of several amino acids of mass less than 450 Da; however, for larger molecules (in the range of the tryptic peptides habitually analyzed in proteomics, from 700 to 4,000 Da), we could not obtain signal when matrix was only composed by graphene. So, it fails to detect any of the 6 peptidic calibrators routinely employed in reflector mode: 4700 Proteomics Analyzer Calibration Mixture (Calmix) with masses in the range between 904 and 3,657 Da. This situation was reverted by adding onto the same spots in the MALDI plate 1 μl of the matrix CHCA, commonly used with these calibrators. In fact, an improvement of the signal intensities, signal to noise ratios and resolution was observed. Therefore, we decided to study the best conditions to optimize spectra acquisition by combining graphene and CHCA.

Loading of matrices and samples

The adequate addition order for the two matrices and the sample was studied. Four different loading combinations (A-D) were prepared with graphene, CHCA and Calmix as sample. In all conditions the volume ratio of graphene:CHCA:Calmix 1:0.5:0.5 (μl) was kept constant. In condition A, the three components were previously mixed and vortexed in a tube and then loaded in the MALDI plate. In condition B, graphene and sample were previously mixed and vortexed, then loaded and allowed to dry, and finally CHCA was added. In condition C, the

graphene was mixed and vortexed with the CHCA, loaded and allowed to dry; the sample was added as the last component. In condition D, graphene was loaded, allowed to dry; then the sample and the matrix were mixed in a tube, vortexed and finally loaded onto the graphene layer.

It was observed that the fourth loading protocol (D) gives the best results with a higher signal than CHCA used alone. In bars **a** and **d** of figure 1 it can be observed the difference of both signals with the loading amounts of the matrices optimized. The signal increases in an order of magnitud. The other tested loading conditions give worse results even than CHCA alone, therefore all the following experiments were carried out using the loading procedure D.

The combination graphene/CHCA not only increases the signal of Calmix compared to the measurement accomplished only with CHCA but also lowers the laser intensity needed to ionize the sample. No signal was observed using only CHCA as matrix for laser intensities below 2700 (arbitrary units), while we were able to detect the signal with graphene/CHCA at a laser power of 2500.

Different ratios of graphene:CHCA as matrices were subsequently tested using Calmix as the sample. Under the experimental conditions described in figure 1, the best result was obtained loading 1 μl of graphene and 1 μl of CHCA.

Sinapinic acid was also evaluated as a co-matrix with graphene with the same loading protocol set up for CHCA. In this case the sample was the calibration mixture 3 of the Sequazyme Peptide Mass Standard Kit (ABSCIEX). In figure 4S of supplemental information it can be seen that the signal was equally enhanced

approximately two times when compared with the response of the sinapinic acid alone.

Utility of the graphene/CHCA matrix for complex samples

A digestion of a complete protein extract derived from human leukocytes was studied by MALDI-TOF/TOF to evaluate the usefulness of the combination graphene/CHCA to analyze complex samples.

Initially, we have to emphasize that an increase of 400 units of the laser intensity was required to obtain a similar spectrum signal with the CHCA matrix alone than with the combination graphene/CHCA (figure 2). Nevertheless, the big difference of peaks detected with lower laser intensity was partially corrected at higher laser intensities. With the combination graphene/CHCA we managed to detect a higher number of peaks than using only CHCA at any laser intensity. A 30% increase in the number of peaks detected was observed in the best spectra of both analyses conditions (graphene/CHCA with laser intensity 3500 and CHCA with laser intensity of 3700). That peaks detection enhancement was observed mainly in the high mass range (figure 3S, Supplemental information) and the resolution of the spectra was significantly improved in this range. The higher rate of peptide fragmentation above 3700 units of laser intensity can explain the decreased amount of peaks detected from this point upwards with both graphene/CHCA and only CHCA matrices (results not shown).

We have observed that the loading conditions of the samples set up using calmix as sample are not always suitable for more complex samples or for samples with

interfering substances. In these cases should first be studied the conditions under which are obtained a better signal. However, in order to have a clearer presentation of the data, the results shown in this article have been always carried out using the protocol D described in the paragraph *Loading of matrices and samples* of this *Results* section.

PSD and CID fragmentation

Two different MS/MS modes are commonly used in MALDI-TOF/TOF mass spectrometers. In PSD (post source decay) MS/MS mode fragmentation is achieved when the excess of vibrational energy obtained at high laser intensities is dissipated by molecular breakdown. In CID (collision induced dissociation) a cell located in the ions path is filled with gas (commonly air) and the fragmentation is achieved by the collision of the analyte molecules with those that fill the cell. As we can see in figure 3, the signal improvement with the use of graphene/CHCA is higher when CID on mode was employed (53,4% ± 12,5 CI 95%) in contrast with PSD MS/MS mode (30,4% ± 12,5% CI 95%.). This also corroborates that graphene facilitates the analyte ionization that can be achieved with lower energy collisions between the molecules of matrix and analyte.

Nanoclusters analysis

To support the idea that the accomodation of the analyte molecules in the graphene planar layers has relevance with regard to its ability to facilitate the ionizacion process, two types of gold nanoclusters (Au NCs) stabilized by small

polar ligand were analyzed. The Au NCs are an assembly of 10 to 100 atoms with a size < 2 nm exhibiting molecular like properties [21, 17]. The core is formed by a variable number of gold atoms stabilized by an external layer of thiol complexes [22, 23]. The molecular masses distribution of these macromolecules is commonly studied by ESI and MALDI-TOF mass spectrometry employing CHCA or sinapinic acid as matrices [24, 25].

Glutathione and zwitterion thiolate-Au NCs were tested with the matrix graphene/CHCA and with CHCA alone (figure 5S, supplemental information). The use of graphene as co-matrix led to a reduction of the signal intensity and the resolution of the MALDI spectra.

Improved detection of phosphorylated peak by graphene/CHCA matrix

Bearing in mind the attenuating fragmentation effect of graphene, we decided to study samples containing easily fragmented posttranslational modifications, like phosphorylated peptides. In figure 4, we can observe an example where we could not detect an expected phosphorylation with the matrix CHCA. The peak at 1758,9 Da is apparently absent with this matrix; however, it was clearly observed by using the combination graphene/CHCA as matrix. The sequence of the phosphopeptide in peak 1758,9: (ALHSFITPPTT*PQLR , where T* is the phosphorylated residue) was confirmed by MS/MS.

Serial dilutions of the digested casein solution were analyzed. The peaks 1660,7 and 1951,8 in figure 5 correspond to the following sequences of the widely studied tryptic peptides phosphorylated of casein: VPQLEIVPNS*AEER (0 missed cleavage)

and YKVPQLEIVPNS*AEER (1 missed cleavage). Their sequences were confirmed by MS/MS analysis. Both peaks were observed with both matrices without any dilution, but with the dilution 1:10 of the sample the peak 1951,8 are lost with CHCA while it is still clearly seen with graphene/CHCA. It is important to note that this effect was observed when the samples were desalted with ZipTips and was not observed when the samples were not previously desalted.

Discussion

The signal enhancement of different peptides obtained using graphene as co-matrix with CHCA can be explained on the basis of several effects. On one hand, the stabilization induced by the planar structure of the graphene sheets might have an accommodative effect on the peptides adsorbed to the surface. The exceptional optical and thermal properties of the graphene gives rise to a high ionization yield where the analyte molecules get less vibrational excitation and therefore the fragmentation rate during the time of flight is decreased. On the other hand, it cannot be ruled out that the main effect is promoted by interaction with the unlocalized electron charge state of the graphene surface. The fact that the graphene alone can be successfully used as a matrix for small molecules is an argument that supports this idea. The fact that, of all the matrix loading methods studied, only gave positive results the one where the graphene is used as a base on which the sample is deposited on the upper surface supports both hypothesis.

Moreover, the fact that the signal intensity was significantly more increased in the CID than in the PSD fragmentation mode supports the idea that the graphene not

only is able to enhance the ionization rate, but it also has an stabilization effect able to elevate the number of ions that reach the detector. Our findings are in agreement with Liu et al [4] who first suggested the attenuating effect of Graphene on the spontaneous fragmentation of molecules flying toward the detector. This attenuation of the fragmentation rate could explain, at least partially, the enhancement of the signal obtained in mode MS. Moreover, it can explain the signal improvement is not uniform in the whole spectrum, because we have more enhancements in those peaks that correspond to molecules that are easily cleavable. Experiments carried out in this work with phosphorylated peptides support also this hypothesis. We showed that the detection is enhanced by the use of graphene/CHCA to the point that we can see phosphorylated peptides that were not observed with only CHCA as matrix. The most plausible explanation for this lies primarily in this stabilizing effect of the graphene.

The worsening of the signal in the analyses of the Au NCs may be due to the fact that the molecules of glutathione and zwitterion cannot be accomodated perfectly flat on the graphene because they are attached to the gold particles so that is impeded by the geometry and the large size of the Au NCs (5-25kDa). Further studies with smaller clusters of few atoms (Au with n<25) or with longer thiolated molecules that can better accommodate on the flat graphene sheets would be of interest to determine if graphene is a suitable matrix to study Au NCs.

The enhancement of the signal with the combination graphene/CHCA is especially useful in the case of complex samples where an increment of 30% in the number of peaks detected was obtained, mainly in the high mass range of the spectra. In Maldi the analyte ionization is gotten by collisions with the matrix molecules

excited/ionized by the laser. Thus, the ionization rate is decreased with larger molecules that have more degrees of freedom to dissipate the energy of the collisions. Due to the same reasoning, the fragmentation of the larger molecules is more difficult. In this sense, the increase of the number of peaks detected in complex samples it can be explained not only due to a charge transfer facilitated on the surface of the graphene but also because of the stabilization effect over the graphene surface that would be able to restrict the degrees of freedom of the molecules that lay down on it.

We consider worthy for further studies to test the use of graphene coated MALDI plates or even plates completely made of this substance. In these conditions might be avoided the undesirable aggregation of the graphene [4], which may significantly reduce the desorption/ionization efficiency. The small molecules perhaps could be analyzed without addition of matrix and the bigger molecules would be analyzed cocrystallized with the differents matrices in the usual way.

In spite of exhibiting a frequency-independent light absorption over a broad spectral region in the visible and infrared, graphene has a characteristic band in the range 250-290 nm (figure 1S and 2S of supplemental information). The use of the graphene as matrix was described in mass spectrometers pumped with a laser emitting at 337 nm (pulsed nitrogen laser) [8] or 355 nm (Nd:YAG laser) [2, 4] which is far from the maximum absorption wavelength of graphene (270 nm) [13]. In these cases the processes involved in the ionization of the molecules must be related to surface electronic charge events, rather than a resonant absorption of light, as it is the case with the traditional matrices used in MALDI-TOF mass spectrometers. In this sense, it would be of great interest the design of

experiments with the use of a laser emitting in this wavelength interval (250 – 290 nm) to test the performance of this novel matrix with a resonant absorption of light.

The use of graphene as matrix was first published in 2010 [8]. Since then, other articles has described the use of graphene as Maldi-TOF matrix [3, 5, 6, 7] and the present work is the first study where the graphene is used as a MALDI adjuvant co-matrix improving ionization rate and having a stabilizing effect that reduce the rate of fragmentation and gives rise to a better detection of phosphorylated peptides and a higher number of peaks detected in the analysis of complex samples.

Acknowledgements

This work was realized thaks to the collaboration of the Proteomics Unit of the SCBI, University of Málaga and was supported by Grants SAF2011-26518 (MINECO, Spain), SAF2010-20203 (MINECO Spain) and CVI-06585 (PAIDI, Andalusia). CIBERER is an initiative of Institute de Salud Carlos III. The authors thankfully acknowledge the expertise understanding and assistance of the Therapeutic Nanosystem, Andalusian Centre for Nanomedicine and Biotechnology (BIONAND) as well as of the Nanotech Unit of the SCBI, “Parque Tecnológico de Andalucía”, Málaga, Spain.

Creo que deberíamos llevar el manuscrito a Norma para que le edite el inglés aunque aún es pronto, es mejor que todos los autores hayan hecho sus enmiendas.

Figure legends:

Figure 1. Calmix spectra were obtained with 5 different ratios graphene/CHCA. 1 μL of Calmix was employed and the same laser intensity (2900) in all tested conditions: a) 0 μl Graphene + 1 μl CHCA, b) 0.25 μl Graphene + 1 μl CHCA, c) 0.5 μl Graphene + 1 μl CHCA, d) 1 μl Graphene + 1 μl CHCA, e) 1 μl Graphene + 0.5 μl CHCA, f) 1 μl Graphene + 0.25 μl CHCA, g) 1 μl Graphene + 0 μl CHCA.

Figure 2: Evolution of the signal in a complex sample: Protein extract of isolated leukocytes was digested with trypsin and the spectra was obtained increasing the laser intensities from 2900 to 3700 with CHCA or graphene/CHCA as matrices.

Figure 3: Comparison of the signal intensities obtained with CHCA and Graphene/CHCA of MS/MS spectra carryed out with CID off and CID on modes.

Figure 4: Improved detection of a phosphorylated peptide. Murine KSR1 (Kinase suppressor of Ras 1) treated with 20 ng MAPK (mitogen-activated protein kinase, see methods) was studied with both matrices. The top spectrum is representative of those obtained with CHCA as matrix and the bottom spectrum is representative of those obtained with graphene/CHCA.

Figure 5: Improved detection of casein phosphorylated peptides with graphene/CHCA matrix. The peaks 1660.7 Da and 1951.8 Da correspond to the following tryptic peptides of casein phosphorylated: VPQLEIVPNS*AEER (0 missed cleavage) and YKVPQLEIVPNS*AEER (1 missed cleavage).

Supplemental information:

Figure 1S: Comparison between spectrophotometric graphene absorption in the range 200 – 500 nm after sonication in either plastic or glass tubes.

Figure 2S: Study of the sedimentation of graphene. Comparison between spectrophotometric graphene absortion in the range 200 – 500 nm after sonication in glass tubes under the following conditions: non sedimented, measurement just after sonication; sedimented, sample resting 45 min on the top bench after sonication; centrifugated, forced sedimentation by centrifugation (1 min at 14000 RCF).

Figure 3S: Spectrum detail in the 2600 - 2850 m/Z range of the figure 2.

Figure 4S: Comparison of the signal intensities obtained with sinapinic acid and Graphene/sinapinic acid of linear mode MS spectra using a sample with 3 proteic calibrators of masses 5734, 11674 and 16952 Da.

Figure 5S: Au-NCs analyzed with CHCA and graphene/CHCA as matrices. a) AuGSH NC, gold nanocluster stabilized by glutathione. b) AuZW NC, gold nanocluster stabilized by a zwitterionic bidentate ligand:

3-((3-(5-(1,2-dithiolan-3-yl)pentanamido)propyl)dimethylammonio)propane-1-sulfonate

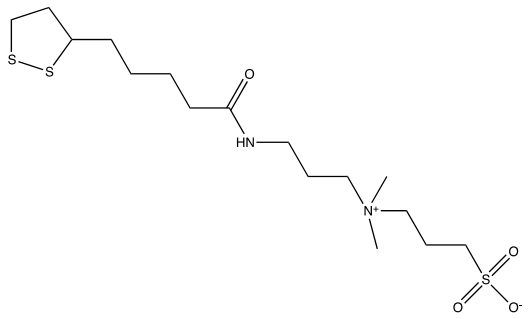

Zw

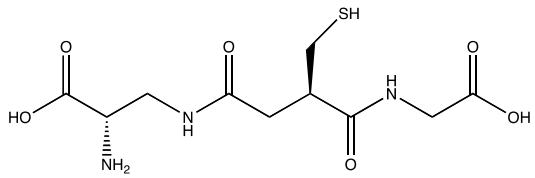

GSH

References

1. Liu J, Liu Y, Gao M, Zhang X. High throughput detection of tetracycline residues in milk using graphene or graphene oxide as MALDI-TOF MS matrix. J Am Soc Mass Spectrom 2012;23(8):1424-7.
2. Wan D, Gao M, Wang Y, Zhang P, Zhang X. A rapid and simple separation and direct detection of glutathione by gold nanoparticles and graphene-based MALDI-TOF-MS. J Sep Sci 2013;36(3):629-35.
3. Shi C, Meng J, Deng C. Enrichment and detection of small molecules using magnetic graphene as an adsorbent and a novel matrix of MALDI-TOF-MS. Chem Commun (Camb) 2012;48(18):2418-20.
4. Liu Y, Liu J, Deng C, Zhang X. Graphene and graphene oxide: Two ideal choices for the enrichment and ionization of long-chain fatty acids free from matrix-assisted laser desorption/ionization matrix interference. Rapid Commun Mass Spectrom 2011;25(21):3223-34.
5. Zhang J, Dong X, Cheng J, Li J, Wang Y. Efficient analysis of non-polar environmental contaminants by MALDI-TOF MS with graphene as matrix. J Am Soc Mass Spectrom 2011;22(7):1294-8.
6. Liu Y, Liu J, Yin P, Gao M, Deng C, Zhang X. High throughput identification of components from traditional chinese medicine herbs by utilizing graphene or graphene oxide as MALDI-TOF-MS matrix. J Mass Spectrom 2011;46(8):804-15.
7. Zhou X, Wei Y, He Q, Boey F, Zhang Q, Zhang H. Reduced graphene oxide films used as matrix of MALDI-TOF-MS for detection of octachlorodibenzo-p-dioxin. Chem Commun (Camb) 2010;46(37):6974-6.
8. Dong X, Cheng J, Li J, Wang Y. Graphene as a novel matrix for the analysis of small molecules by MALDI-TOF MS. Anal Chem 2010;82(14):6208-14.
9. Mak K,Fai, Ju ,Long, Wang ,Feng, Heinz T,F. .
10. Bonaccorso ,F.\, Sun ,Z.\, Hasan ,T.\, Ferrari A,C.\. Graphene photonics and optoelectronics\. .
11. Chang ,Haixin, Tang ,Longhua, Wang ,Ying, Jiang ,Jianhui, Li ,Jinghong. .
12. Park ,Sungjin, An ,Jinho, Potts J,R., Velamakanni ,Aruna, Murali ,Shanthi, Ruoff R,S. .
13. Liu Q, Cheng M, Jiang G. Mildly oxidized graphene: Facile synthesis, characterization, and application as a matrix in MALDI mass spectrometry. Chemistry 2013;19(18):5561-5.
14. BOYUM A. Separation of white blood cells. .
15. Houthaeve T, Gausepohl H, Ashman K, Nillson T, Mann M. Automated protein preparation techniques using a digest robot. J Protein Chem 1997;16(5):343-8.
16. Ashman ,Keith, Houthaeve ,Tony, Clayton ,Jonathan, Wilm ,Matthias, Podtelejnikov ,Alexandre, Jensen ,OleN., et al. The application of robotics and mass spectrometry to the characterisation of the drosophila melanogaster indirect flight muscle proteome. .
17. Guevel XL, Tagit O, Rodriguez CE, Trouillet V, Pernia Leal M, Hildebrandt N. Ligand effect on the size, valence state and red/near infrared photoluminescence of bidentate thiol gold nanoclusters. Nanoscale(14):8091.
18. Bolotin KI, Sikes KJ, Jiang Z, Klima M, Fudenberg G, Hone J, et al. Ultrahigh electron mobility in suspended graphene. Solid State Commun 2008;146(9–10):351-5.
19. Balandin AA, Ghosh S, Bao W, Calizo I, Teweldebrhan D, Miao F, et al. Superior thermal conductivity of single-layer graphene. Nano Lett 2008;8(3):902-7.
20. Park J, Nam J, Won N, Jin H, Jung S, Jung S, et al. Compact and stable quantum dots with positive, negative, or zwitterionic surface: Specific cell interactions and non-specific adsorptions by the surface charges. Advanced Functional Materials 2011;21(9):1558-66.
21. Zheng J, Nicovich PR, Dickson RM. Highly fluorescent noble-metal quantum dots. Annu Rev Phys Chem 2007;58:409-31.
22. Angel LA, Majors LT, Dharmaratne AC, Dass A. Ion mobility mass spectrometry of Au25(SCH2CH2Ph)18 nanoclusters. ACS Nano 2010;4(8):4691-700.
23. Negishi Y, Nobusada K, Tsukuda T. Glutathione-protected gold clusters revisited:â€‰ bridging the gap between gold(I)âˆ’Thiolate complexes and thiolate-protected gold nanocrystals. J Am Chem Soc 2005;127(14):5261-70.
24. Chaudhari K, Xavier PL, Pradeep T. Understanding the evolution of luminescent gold quantum clusters in protein templates. ACS Nano 2011;5(11):8816-27.

25. Harkness KM, Cliffel DE, McLean JA. Characterization of thiolate-protected gold nanoparticles by mass spectrometry. Analyst 2010;135(5):868-74.
26.